

Supplemental Information

Supplemental Figure Legends

Supplemental Figure 1. **A**, Detection of GFP-LC3 clusters in HEK 293 cells expressing GluD2^{Lc}. Left, raw image. Right, image after applying a linear filter and an object detection algorithm (IPLab Spectrum 3.6; Signal Analytics, Vienna, VA). Scale bar, 10 μm . **B, C**, Analysis of cell death by propidium iodide (PI) staining. HEK 293 cells were cotransfected with cDNAs encoding EGFP and GluD2^{wt}, GluD2^{Lc}, GluD2^{Lc}-Q618R, GluD2^{Lc}-V617R, GluD2^{wt}- Δ ACT7, or GluD2^{Lc}- Δ ACT7. At 15 h after transfection, the cells were stained with PI. Representative images are shown in (B). The percentage of EGFP-positive cells stained for PI is shown in (C). The values represent the mean \pm SEM from 3 independent experiments. ** $p < 0.01$.

Supplemental Figure 2. EGFP-Becclin1 clustering and decreased cellular ATP levels were regulated by extracellular Na⁺ concentrations in cells expressing GluD2^{Lc}. **A**, Representative fluorescence images of HEK 293 cells expressing EGFP-Becclin1 and either GluD2^{wt} or GluD2^{Lc}. **B**, Effect of extracellular Na⁺ concentrations on EGFP-Becclin1 clustering and cellular ATP levels. HEK 293 cells were cotransfected with EGFP-Becclin1 and GluD2^{Lc}. At 6 h after transfection, the culture medium was changed to the artificial cerebrospinal fluid containing various Ca²⁺ concentrations. At 15 h after transfection, the number of EGFP-Becclin1 clusters (left axis) and cellular ATP levels (right axis) were measured. Each point represents mean \pm SEM from 3 independent experiments. Scale bar, 20 μm

Supplemental Figure 3. The deletion of the PDZ-binding motif of GluD2 did not cause cell death *in vivo*. The number of Purkinje cells was quantified in slices prepared from a GluD2^{wt}- Δ CT7 line (that expressed a mutant GluD2 transgene lacking the C-terminal seven amino acids on a *GluD2*-null background) and a GluD2^{wt} line (that expressed a wild-type GluD2 transgene on a *GluD2*-null background) at approximately 5 postnatal weeks. Although the region deleted in a GluD2^{wt}- Δ CT7 line is essential for binding to PDZ proteins such as n-PIST, no significant (n.s.) Purkinje cell loss was observed. The values represent the mean \pm SEM of three slices. n.s., no significance. Scale bar, 200 μ m

Supplemental Figure 4. Morphology of cerebellum of *Lc/+* mice on an *Atg5*-null background at P10. Representative gross morphology (top panels) and immunohistochemical analysis of parasagittal sections of cerebellum using anti-calbindin and anti-synaptophysin (presynaptic marker) antibodies (middle, cerebellar cortex; bottom, deep cerebellar nucleus [DCN] region) are shown. The arrowheads in the middle panels represent the loss of Purkinje cells in the cerebellar cortex. The arrows in the bottom panels represent the swollen axons of Purkinje cells in the DCN region. Scale bars, 20 μ m in the middle panels and 100 μ m in the bottom panels.

Supplemental Figure 5. Swelling of HEK 293 cells expressing GluD2^{Lc} during the early phase of cell death. HEK 293 cells expressing GluD2^{Lc} and EGFP were continuously perfused with ACSF and imaged between 6 h and 14 h after transfection.

Images were taken every 10 min. **A**, Representative phase contrast images of HEK 293 cell. Red arrows indicate an EGFP-positive cell expressing GluD2^{Lc}. **B**, Estimation of the volume of cells expressing mock or GluD2^{Lc}. The maximum cell areas were measured between 6 h and 14 h after transfection. Each cell area was plotted as black circle (control) or red diamonds (GluD2^{Lc}). The averaged cell areas were shown as black bar (control) and red bar (GluD2^{Lc}). The results were from 3 independent experiments. ** $p < 0.01$.

Supplemental Figure 6. Proposed model of GluD2^{Lc}-induced autophagy and cell death. Intracellular ATP levels are decreased probably by overstimulation of ATP-dependent pumps, such as Na⁺, K⁺-ATPase, in response to constitutive Na⁺ influx through GluD2^{Lc} channels. Decreased ATP levels are sensed by AMPK, which activate autophagy via inhibition of mTOR. Ion overload induces persistent cell swelling, and together with decreased ATP levels, causes necrotic cell death. Secondary Ca²⁺ influx through voltage-gated Ca²⁺ channels will also activate various Ca²⁺-dependent degradative enzymes and contribute to cell death. Association of n-PIST–Beclin1 with the C-terminus of GluD2 may not be directly involved in unlikely contribute to GluD2^{Lc}-induced autophagy and cell death.

Supplemental Movie

Supplemental Movie 1. HEK 293 cells expressing GluD2^{Lc} became swollen before cell death.

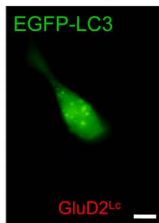
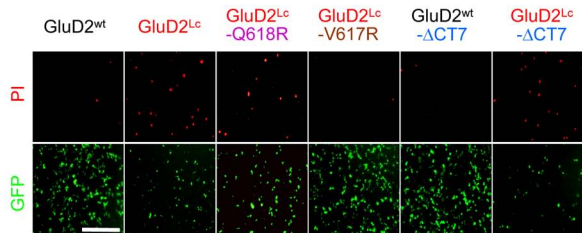
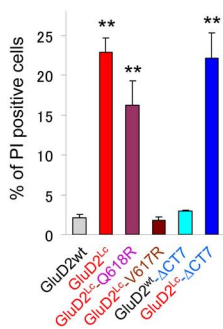
Supplemental Movie 2. Behaviors in Lc/+; *Atg5*^{+/+} and Lc/+; *Atg5*^{-/-} mice. Both

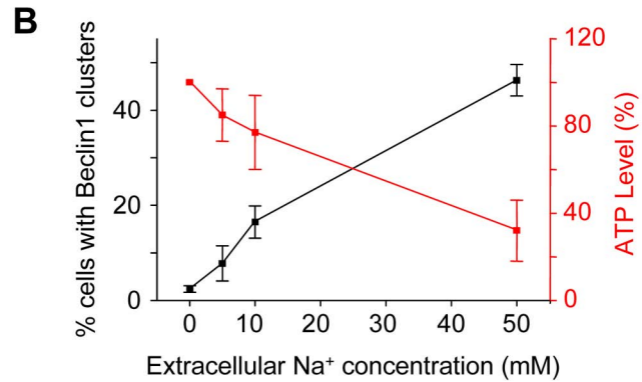
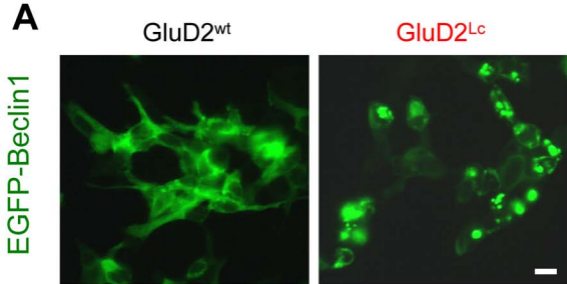
mice showed similarly severe ataxia movement at P18.

A

raw image

filtered image

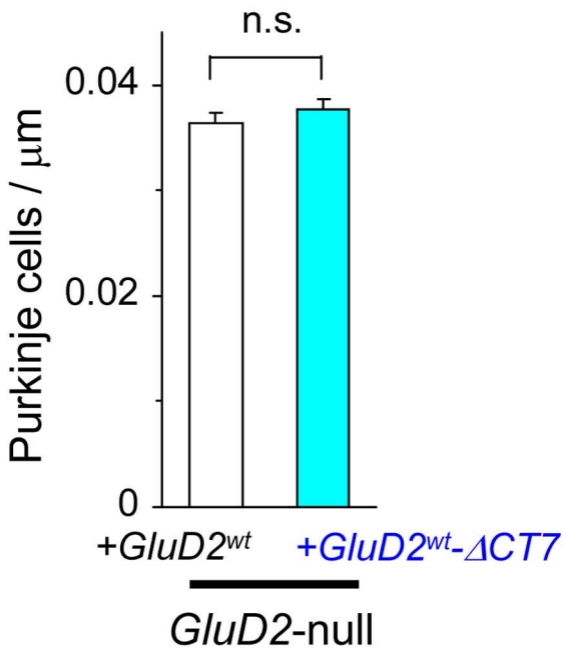
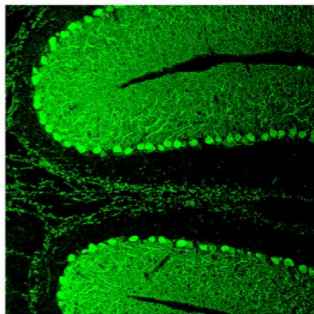
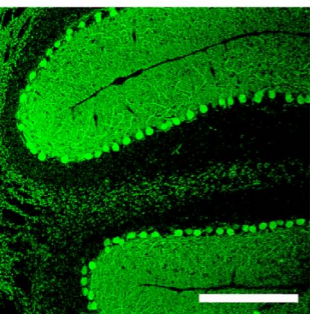
**B****C**



GluD2-null

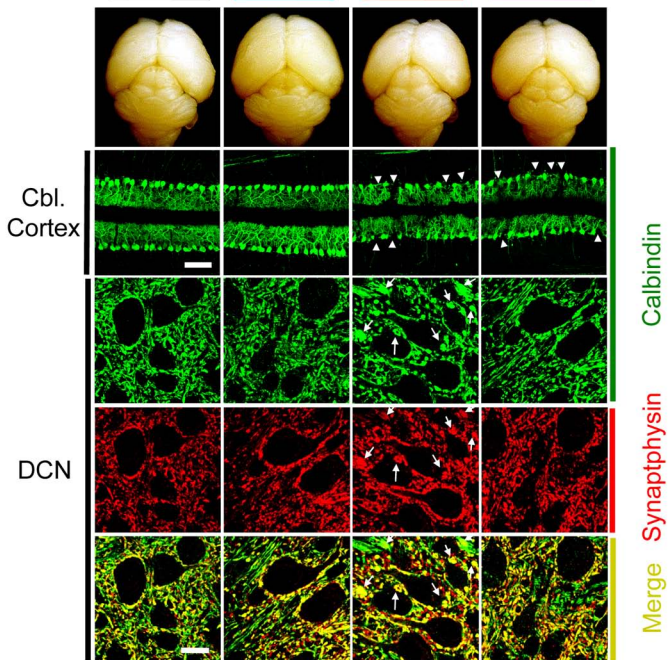
+*GluD2*^{wt}

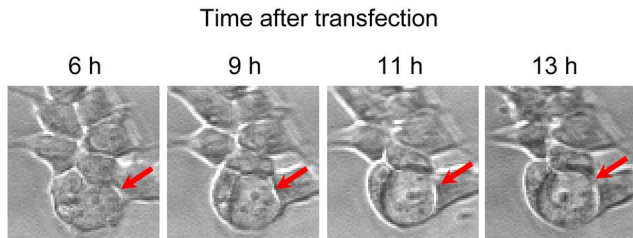
+*GluD2*^{wt}- Δ CT7



P10

Lc: +/+ +/+ Lc/+ Lc/+
Atg5: +/+ -/- +/+ -/-



A**B**